

Electrochromic Nickel Oxide Films for Smart Window Applications

Michelle P. Browne*, Hugo Nolan, Nina C. Berner, Georg S. Duesberg, Paula E Colavita and Michael

E. G. Lyons*

School of Chemistry and CRANN, Trinity College Dublin, The University of Dublin, College Green, Dublin 2, Ireland

*E-mail: melyons@tcd.ie, brownem6@tcd.ie

Received: 13 May 2016 / Accepted: 2 June 2016 / Published: 7 July 2016

In this study, nickel oxide films were prepared through an electrodeposition technique. NiO films were fabricated on Indium Tin Oxide (ITO) supports by cycling the potential between two different sets of limits. The electrodeposition technique which involved using the shorter potential limits was denoted as deposition process 1 and the technique using the wider potential limits was called deposition process 2. Subsequently, the films fabricated by the two deposition process were evaluated as electrochromic materials. The results show that the Colouration Efficiency (CE) values achieved for the deposition process 1 and 2 were $49 \text{ cm}^2 \text{ C}^{-1}$ and $10 \text{ cm}^2 \text{ C}^{-1}$, respectively. The switching times of the film made by the first deposition process were also calculated, as this film showed improved electrochromic capabilities. The coloration and bleaching switching times for this NiO film are 5.7 and 7.4 seconds, respectively. The improved electrochromic results for the film fabricated by deposition process 1 may be due to the smaller potential deposition window as it produced a thinner film with no traces of sulphate ions on the film's surface compared to the other NiO film produced by the second electrodeposition technique. The films are characterized by SEM-EDX, Raman spectroscopy and XPS. The regeneration of the bleach state was shown to be hindered. This may be due to conductive pathways involved in the reduction of the coloured state being blocked. Raman spectroscopy was used to determine the presence of both the $\text{Ni}(\text{OH})_2$ and NiOOH after the reduction event.

Keywords: Electrochromic, Nickel Oxide, Electrodeposition, Bleached, Coloured, Raman, XPS.

1. INTRODUCTION

Electrochromic materials have the ability to change colour in the presence of an external voltage. This phenomenon is governed by the intercalation and de-intercalation of small ions into and out of the material layers.[1, 2] These materials have potential applications in smart windows and

smart devices, due to their low power consumption and high coloration efficiency (CE).[3, 4] The development of this technology may lead to a significant reduction in energy consumption in homes and offices due to the decrease in heating and cooling cost, particularly in glazed buildings. In their bleached state these material can allow light and heat pass through them however this is the opposite when these materials are in its coloured state.

Smart windows are made from a five layered sandwich-like device inside a pane of glass. This device consists of a transparent conductor (TC) on either end of the device with a solid electrolyte/ionic conductor (IC) in the middle with a counter electrode between a TC and IC on one side. On the other side of the device between another TC and IC lies the active/primary electrochromic material. This is the layer that is responsible for the colour change within the device.

Transition Metal Oxides or TMO's are widely used in electrochemical energy applications e.g. Supercapacitors,[5-7] water splitting catalysts [8-10] and fuel cell catalysts, [11, 12] therefore it is no surprize that TMO's are also a good candidate for electrochromic materials.[13, 14] Nickel oxide shows great promise as an active electrochromic material. Nickel oxide is a cheap, abundant and can be easily fabricated. Upon applying a potential of approximately 1.35 V (vs. RHE) and greater, the transparent Ni oxide transforms into a dark brown Ni oxide, otherwise known as the bleached and coloured state respectively. It is generally accepted that the cause of this coloration is due to the Ni (II) to Ni (III) redox process in alkaline media. [1, 15]

Electrochromic NiO films have been previously prepared by a variety of different methods including sol-gel[16], chemical vapour deposition[4], sputtering[17] and electrodeposition[15]. In this work, an electrodeposited procedure will be implemented for the fabrication of electrochromic thin films. In this study, the nickel oxide films will be produced by multi-cycling a nickel sulphate solution at different lower limits. The effects of the changing of this lower limit on the materials optical performance will be investigated. Spectro-electrochemical techniques will be used to determine the optical properties (Transmittance) of the films. Subsequently, the coloration efficiency will also be calculated. The resulting NiO films in their coloured and bleached states will be characterised by XPS, Raman and SEM-EDX.

2. EXPERIMENTAL

All electrochemical experiments were undertaken in a standard three-electrode cell. The electrochemical measurements were performed using a high performance digital potentiostat (CH model 1760 D Bi-potentiostat system monitored using CH1760D electrochemical workstation beta software). Electrochemical measurements were taken at a constant temperature of 25 °C, using a thermal bath with the temperature maintained by a thermostat. All solutions were degassed for 15 minutes before commencing any analysis, to eliminate any dissolved oxygen present in the electrolyte.

The electrodeposition of the NiO thin films onto transparent indium-tin oxide (ITO) films were carried out by cyclic voltammetry using a deposition solution consisting of 0.1 M nickel sulphate, 0.1 M sodium acetate and 0.001 M potassium hydroxide. Two different electrodeposition procedures were carried out during this study. The first deposition, to be termed deposition process 1, was carried out

by multi-cycling the potential between 0.0 V to 1.1 V (vs. Ag/AgCl reference electrode). The second deposition, termed from now on as deposition process 2, was carried out by cycling between the potential limits of -0.9 V to 1.2 V (vs. Ag/AgCl reference electrode). Both depositions were performed at a scan rate of 50 mV dec/s for 25 cycles and a graphite rod was employed as a counter electrode.

Uv-vis in-situ electrochemical measurements were performed using an ALS SEC2000 Uv/visible miniature spectrophotometer with the Visual Spectra 2.1 software. The optical absorption and transmittance spectra of the coloured and bleached states were recorded in the wavelength range of 280-820 nm during polarisation.

All Raman spectroscopy measurements were performed using a Witec alpha 300 R confocal Raman microscope. A 532nm diode laser was used at a power of approximately 10W to irradiate samples. Raman spectra were recorded using a diffraction grating of either 600 or 1800 lines per mm. The morphological characteristics of the NiO on the ITO electrode were determined using a Karl Zeiss Ultra Field Emission scanning electron microscope at an accelerating voltage between 15 KeV - 2 KeV at a working distance of between 7 mm - 1 mm.

XPS measurements were carried out using a VG Scientific ESCALab MKII system using an Al $K\alpha$ X-rays source (1486.7 eV). The sample spot size was approximately 2 mm, meaning a large area of the sample was analysed and spectra are indicative of the whole sample rather than discrete locations. For survey scans, an analyser pass energy of 200 eV was used while a pass energy of 20 eV was used to obtain high resolution spectra of characteristic core levels. The binding energy scale was referenced to the C 1s peak of adventitious carbon at 284.8 eV and the high resolution core level peaks were subsequently fitted using the Casa XPS software.

3. RESULTS AND DISCUSSION

The deposition of the nickel oxide onto the Indium Tin Oxide (ITO) substrate was performed and monitored by cyclic voltammetry, as the current density recorded during repetitive potential sweep conditions increases with increasing growth of the nickel oxide on the substrate, Figure 1(a).

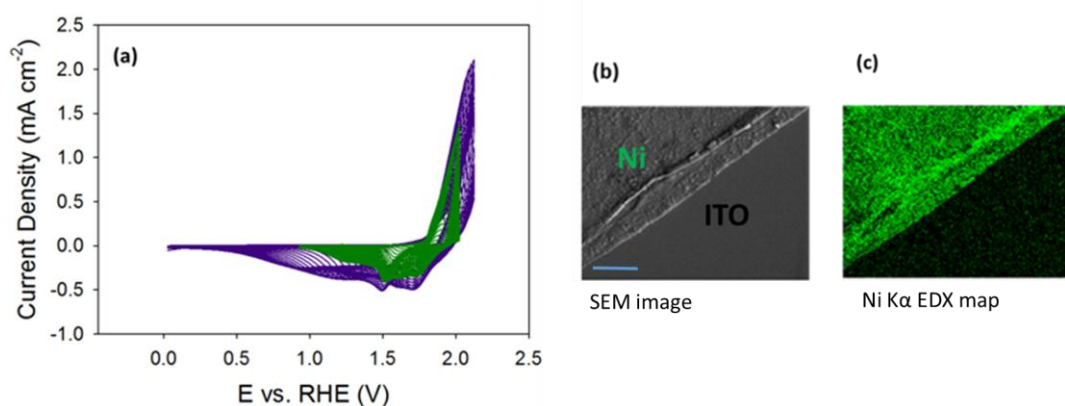


Figure 1. (a) Cyclic Voltammogram of the as-deposited nickel oxide film prepared via deposition process 1 (green) and deposition process 2 (purple) (b) SEM image of the as-deposited Ni oxide (scale bar is 100 μ m)(c) EDX-Mapping of the as-deposited Ni oxide film.

To confirm the presence of nickel on the ITO substrate, EDX mapping was utilised in Figure 1 (b). The raised layer in the electron image was determined to be Ni, as shown in the Ni K α map by the green area, Figure 1(c). The EDX mapping was conducted at the end of the nickel oxide film as this allowed for comparison of a nickel oxide deposited section of the substrate and a bare ITO section. A film thickness's of 100-300 nm was measured for deposition and 1-3 μ m for deposition 2 was measured for the as-deposited films by a profilometer.

Raman spectroscopy was utilised to determine the nickel oxide species formed in the bulk of the bleached and coloured samples resulting from the potential applied. Figure 2(a), shows Raman spectra and (b) SEM images of the electrodeposited nickel oxide films. Each film was grown, as previously described, then immersed in 1M NaOH and the potential of either 0.2 V (bleached) or 0.8 V (coloured) was applied. The film was retrieved from the NaOH solution, washed with H₂O and analysis was conducted.

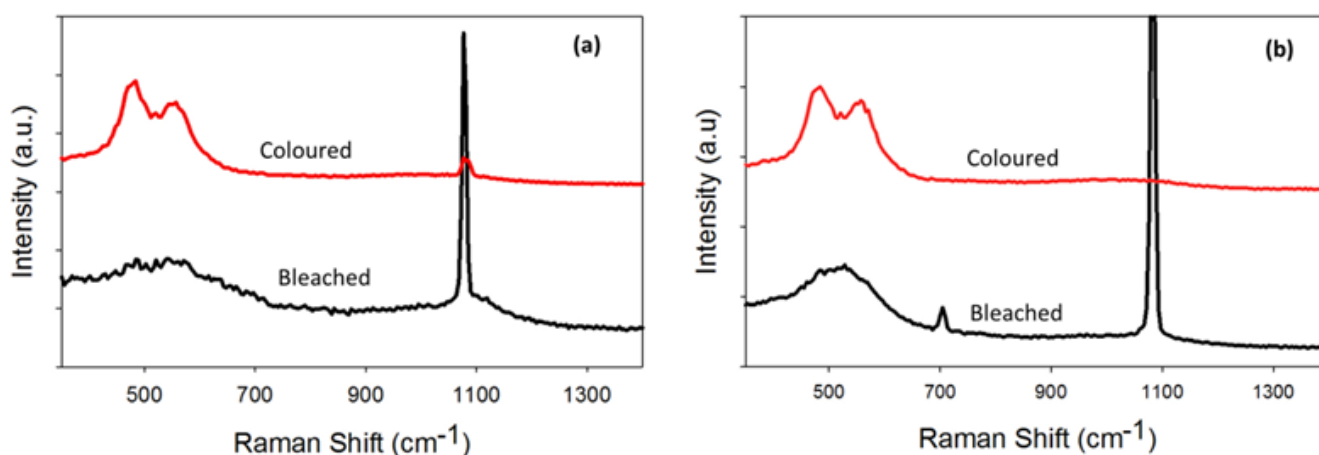


Figure 2. Raman spectra of coloured and bleached states for (a) deposition process 1 and (b) deposition process 2

Previous studies have reported that the Ni(OH)₂ species produces one Raman band in the region of 445-465 cm⁻¹ however, a shift of up to 65 cm⁻¹ can be observed from this region in disorder or doped Ni(OH)₂. [18] The bleached state, at the potential of 0.2 V, contains a Raman peak at 523 cm⁻¹. This band indicates that a disordered Ni(OH)₂ is present. As the deposition solution is made up of nickel sulphate, it is possible that sulphate ions have been inserted into the Ni(OH)₂ lattice during deposition causing the Ni-O vibration of the Ni(OH)₂ to increase in Raman shifts. The band at 1076 cm⁻¹ confirms this, as it can be assigned to the Raman active modes of sulphate ions. The coloured state reveals bands at 471 cm⁻¹ and 550 cm⁻¹ which can be assigned to the Raman active shifts of NiOOH. [19]

Figure 2(b and c), shows SEM images of the electrodeposited nickel oxide in its coloured and bleached states, respectively. A cracked morphology was observed for the nickel oxide film in its bleached state. This cracking in nickel oxide films has been previously reported to be attributed to tensile stress, especially films with a thickness above 0.2 μ m. This explains the morphology of the

nickel oxide film in this study, as the thickness is 1-3 μm . The film became more disordered upon applying a potential in order to change the film into the coloured state. This disordered morphology may be due to the intercalation and de-intercalation of ions in and out of the films surface layers. Characterisation of the nickel oxide at the surface of the two states was carried out by XPS. Subsequently, the elemental differences in the composition of the bulk and on the surface of each of the samples were also investigated.

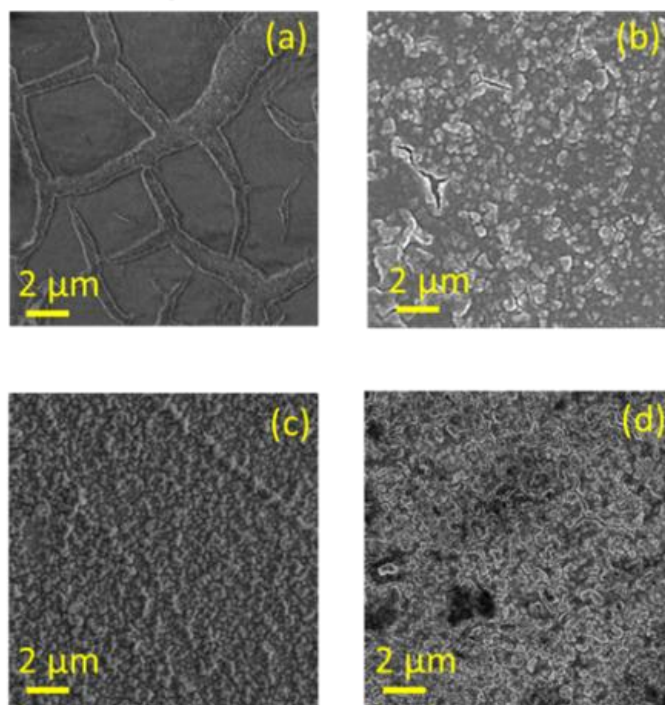


Figure 3. Scanning Electron Images of (a) film formed via deposition process 1 in bleached/resting state (b) deposition process 1 in coloured/active state (c) deposition process 2 in bleached/resting state and (d) deposition process 2 in coloured/active state

XPS survey spectra, Figure 4, clearly illustrate a variation between the surface chemistry of the bleached and coloured states. Each of the spectra contains core level peaks which can be assigned to nickel, oxygen and carbon. The presence of the Na 1s peak, in the bleached and coloured samples, can be easily explained as it is due to the electrolyte, NaOH. Samples are washed before characterisation techniques however electrolyte residue still remains. The In 3d peak for the coloured state increases significantly in intensity compared to the In 3d peak for the as-deposited film and bleached state. This may signify the introduction of indium moieties on the surface of the sample from the substrate due to the loss of some of the nickel oxide film when applying a higher potential. The lack of the S2p peak in Figure 4(b and d) indicates that no sulphate is present on the surface of either of the bleached or coloured samples for both depositions. These sulphate ions on the surface may be freed into the NaOH electrolyte during polarization but still remains in the bulk, as observed in the Raman Spectroscopy, Figure 2.

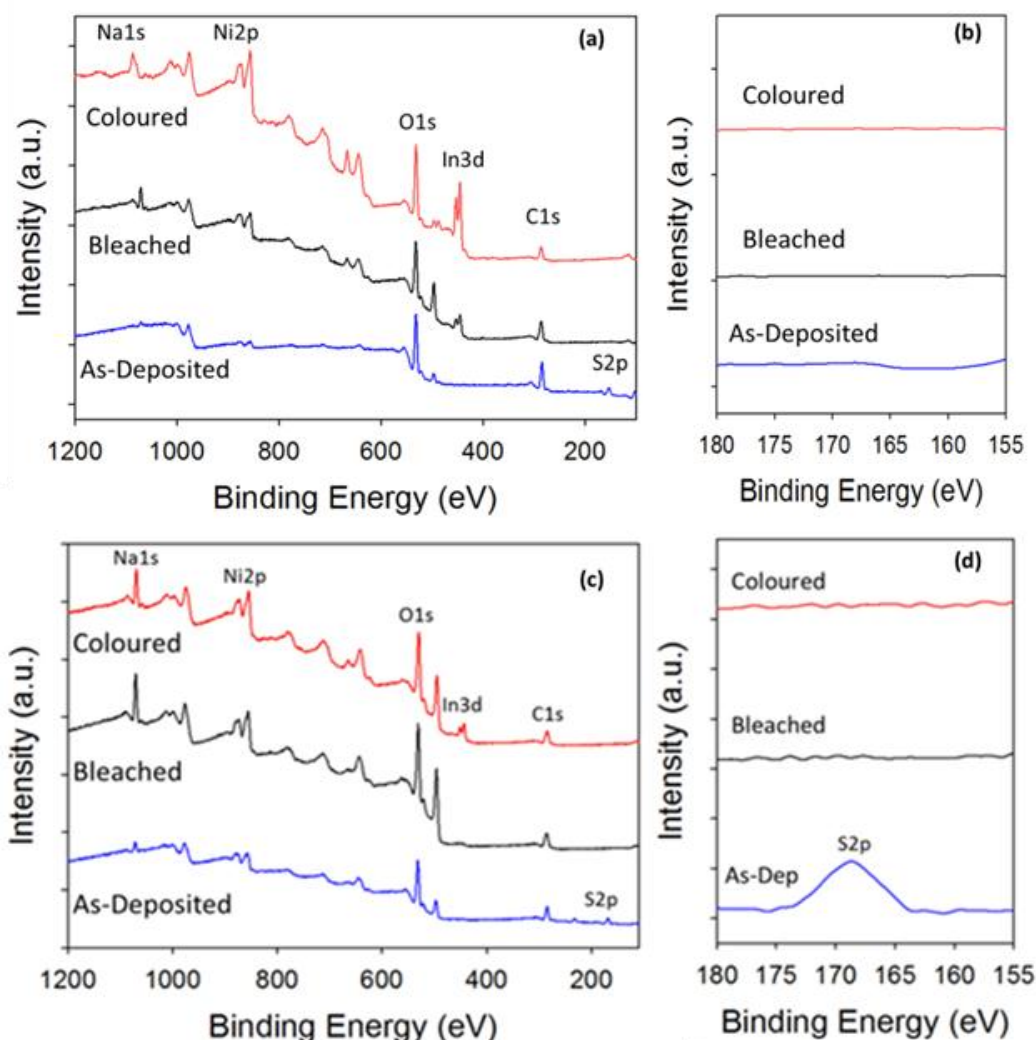


Figure 4. X-Ray Photoelectron survey spectra for (a) deposition 1 (b) deposition 2 (c) survey scan of the Sp2 region for deposition 1 (d) survey scan of the Sp2 region for deposition 2

The sulphate ions observed in the as-deposited sample for the deposition 2 process, Figure 3(d), is more than likely be due to the electrodeposition solution as it contains nickel sulphate as a precursor. The decrease of the S2p core level peak in the XPS survey scan of the sample fabricated by deposition 1 compared to that of deposition 2 is perhaps due to the longer reduction scan enabling more sulphate ions to be deposited onto the ITO electrode with the Ni oxide film. In both depositions, the sulphate is lost after the films are cycled in base, Figure 5(b and d).

High resolution scans of the Ni2p core level peak spectral region allowed contributions to be fitted to each sample. The fitting of these high resolution peaks allows the assigning of various species. The XPS analysis of nickel oxide species has been deemed very difficult due to the complexity of its multiplet splitting and shakes up peaks.[20] The experimental Ni2p_{3/2} core level of the bleached and coloured state samples, for both deposition processes, in Figure 5, were fitted using peak positions and intensities similar to those used by Grosvenor *et al.*[20] For the deposition 2 process, the fits revealed

that the Ni(OH)_2 is assigned to the bleached state while the NiOOH species is found on the surface of the coloured state sample. This correlates with the Raman spectroscopy results for the nickel oxide species found in the bulk. However, the fitting for the bleached and coloured sample for deposition 1, Figure 5(a and b), consisted predominately of Ni(OH)_2 . This result, is rather interesting, the Raman spectra for the coloured state for deposition 1 reveals that the bulk material is oxidized to NiOOH but the XPS shows the surface species of this material stays in the Ni^{2+} state. This may be due to an ageing or memory effect of the film.

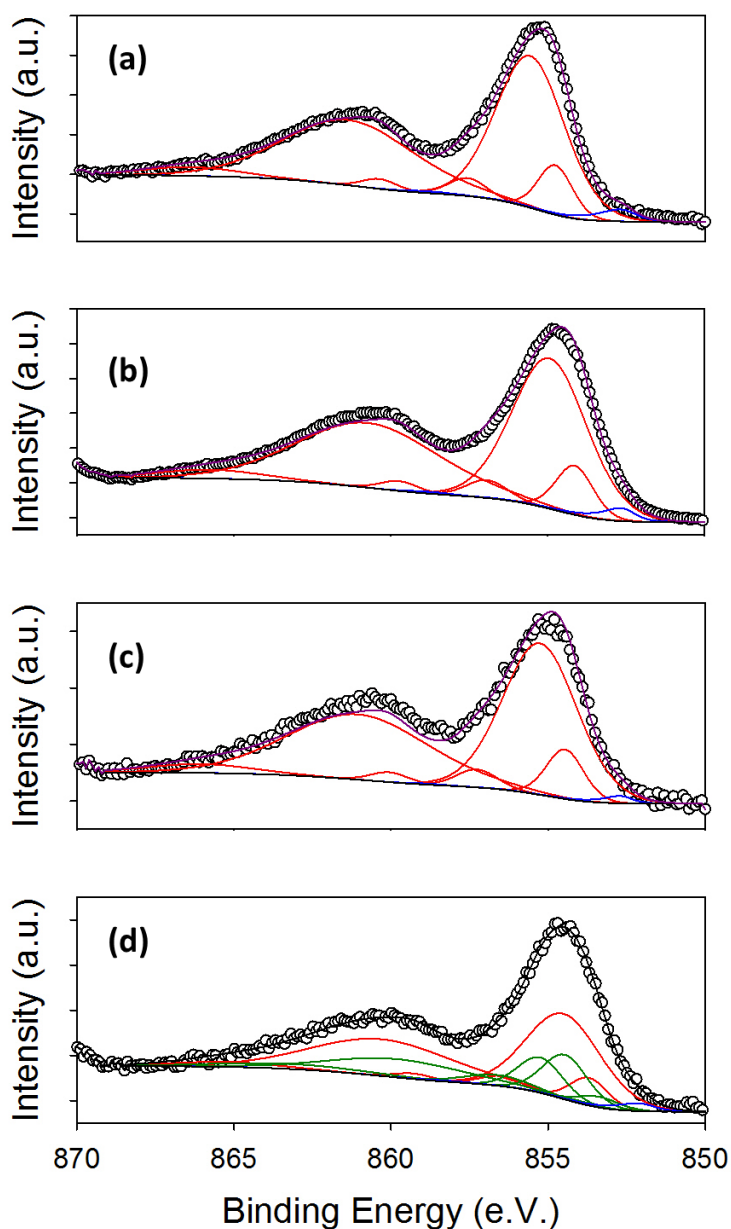


Figure 5. High Resolution X-Ray Photoelectron Spectra of the $\text{Ni}2p_{3/2}$ peak for (a) deposition process 1 – bleached (b) deposition process 1 – coloured (c) deposition process 2 – bleached and (d) deposition process 2 – coloured.

3.1. Electrochromic properties

In-situ spectroelectrochemical experiments were used to evaluate the electrochromic properties of the electrodeposited nickel oxide on the ITO substrate. The colour of the nickel oxide from both of the depositions, in this work, switches from colourless (bleached) to dark brown (coloured) at potentials which are governed by the Ni(II) to Ni(III) redox process in the bulk of the materials, Figure 2 and 6.

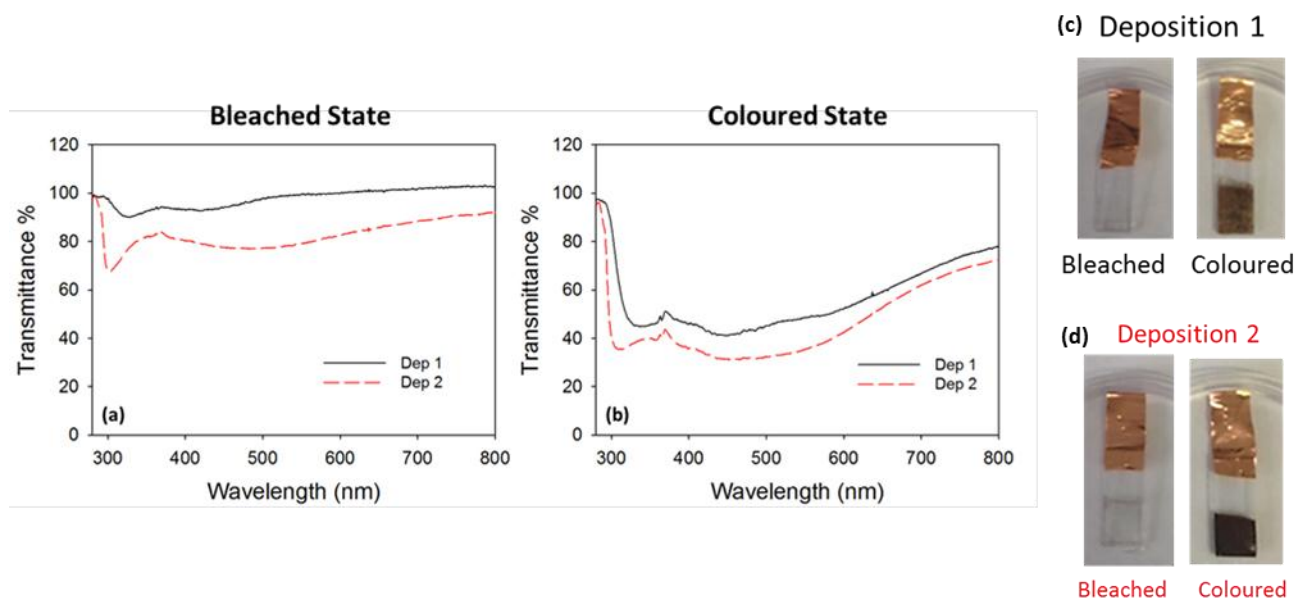


Figure 6. Optical transmittance spectra for the electrodeposited Ni oxide fabricated by deposition process 1 (black) and deposition process 2 (red) in its (a) bleached and (b) coloured states (c) colour of bleached and coloured states from deposition process 1 and (d) colour of bleached and coloured states from deposition process 2.

The change in colour from the bleach state to the coloured state is caused by the intercalation and de-intercalation of the OH⁻ ions into the Ni(OH)₂ and NiOOH layers. The Colouration Efficiency (CE) is the most important parameter for grading the electrochromic performance of a material against other materials. The CE can be defined as the change in optical density per unit charge density.

$$CE = \frac{\Delta OD}{\Delta Q}$$

$$OD = \log(T_b/T_c)$$

T_b and T_c is the transmittance of the bleached and the coloured states respectively. The ΔQ is the difference in charge consumed per unit area, obtained from integrating the area underneath the cyclic voltammogram. The CE calculated for the electrodeposited Ni for deposition process 1 was 49 cm² C⁻¹ while a lower CE value of 10 cm² C⁻¹ was achieved for deposition process 2.

The difference in CE values could be attributed to the mixed Ni(OH)₂/NiOOH species being formed at the surface/bulk of the film fabricated by deposition one and the thinner film, observed in Figure 2 and 5. Another reason for the change in CE could be due to the increase amount of sulphate ions in the deposition 2 film for the as-deposited film, observed in Figure 4(d). Even though the sulphate ions are lost after applying a potential, the effect of this loss may affect the films ability to switch from the different states at the same rate as the film fabricated by deposition 1 with a smaller electrodeposition window. This smaller deposition window allows for no sulphate ions to be inserted into the final film. The larger CE value for the NiO film from the deposition 1 method indicates that this material has a greater change in optical properties for the same electrochemical active area than the NiO produced by method 2. The colouration efficiency achieved by deposition one is extremely comparable with CE values reported in literature for Ni oxides.[12, 13]

To investigate the switching times of the Ni oxide material in this study with the largest CE, in-situ UV-vis and chronoamperometry was utilised. Switching times is defined as the time it takes to reach 90 % of the final change in transmittance when alternating between states. To measure the switching times, a potential corresponding to each state was applied to the material and the current was recorded. The switching times for the Ni oxide film fabricated by deposition one can be observed in Figure 7(b).

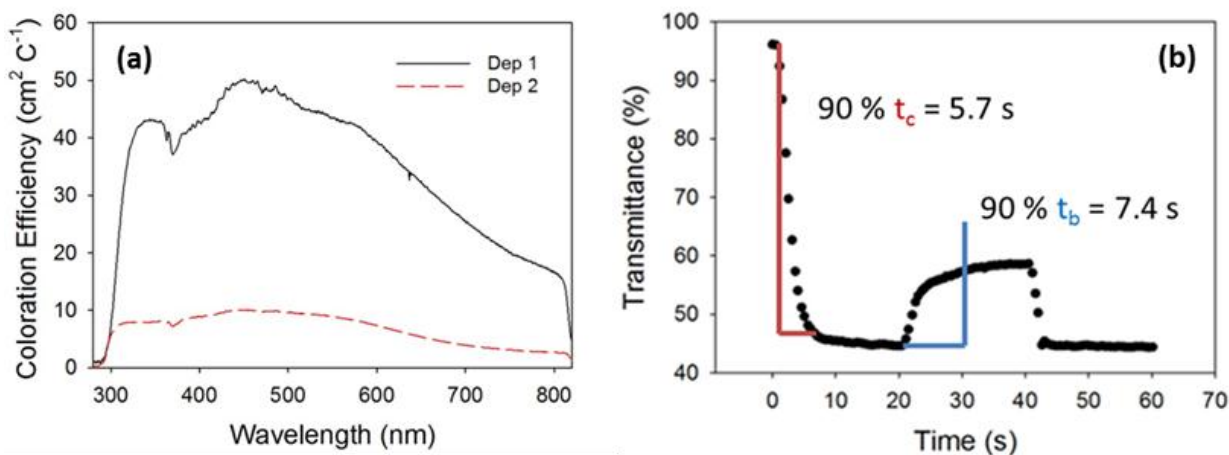


Figure 7. (a) Coloration efficiency (CE) for the electrodeposited Ni oxide fabricated by deposition process 1 (black) and deposition process 2 (red) and (b) Switching times for the Ni oxide film fabricated by deposition 1.

The coloration and bleaching switching times are 5.7 and 7.4 seconds. These t_c and t_b times are faster than those previously reported by *Baek et al.* and *Lin et al.*[13, 21] Unfortunately, the regeneration of the initial transmittance for the bleach state is not restored following colouration therefore further work needs to be done on these Ni oxide materials for electrochromic applications. This can also be observed in Figure 7(b). Raman spectroscopy spot scans were performed on the Ni oxide film after the switching time experiment and revealed the presence of NiOOH and Ni(OH)₂,

Figure 8. Therefore even though the transmittance increased indicating reduction of the NiOOH to Ni(OH)₂, some of the NiOOH remained. This indicates only partial reduction of the Ni^{3+/2+} dark species hence why the transmittance is not restored to 95%. This observation is in good agreement with the shape of the typical cyclic voltammetric response observed in aqueous base for an electrodeposited nickel oxide thin film electrode which has been grown by a potential cycling perturbation (Figure 9). It is clear that the shape of the current/potential profile for the anodic sweep is much sharper than that observed for the reverse cathodic sweep, indicating that layer oxidation is more rapid than layer reduction. This observation is in agreement with percolation theory. Clearly the current increases sharply during the anodic sweep once the percolation threshold is attained since electronic connectivity is established throughout the deposited film. In contrast for the reduction process conductive pathways within the film are cut and there may be significant regions of oxidized sites remaining within the layer at reducing potentials. In table 1 we summarize the relevant KPI's for the nickel oxide thin films prepared in the present work and compare these with literature values. We note that the CE depends markedly on the potential limits used in the deposition process. Hence we conclude that the electrochromic properties of the oxide material will be a strong function of the synthetic route employed.

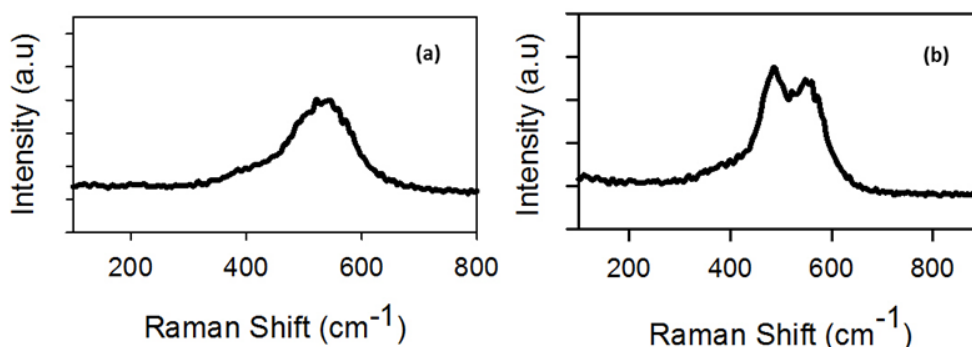


Figure 8. Raman analysis of the Ni oxide film produced by deposition process 1 after time switching experiments.

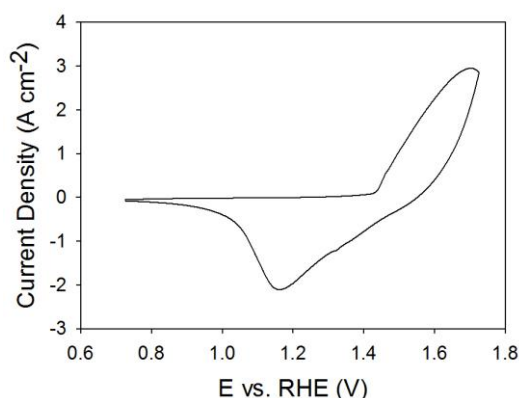


Figure 9. Typical CV for the NiO film produced by the deposition 1 process

Table 1. Comparison of Key performance indicators for the Ni oxide films fabrication in this work with literature values.

Name	T _B (%)	T _C (%)	ΔT	CE (cm ² C ⁻¹)	T _c (s)/ t _b (s)	Ref
Dep 1	95	45	50	49	5.7/7.4	This work
Dep 2	80	35	45	10	n/a	This work
Ni oxide FTO	56	26	30	21	n/a	[22]
Ni oxide ITO	n/a	n/a	n/a	42	15/5	[23]
Conventional Ni	n/a	n/a	n/a	25.5	6.5/12	[21]

4. CONCLUSIONS

Two electrochromic NiO materials were fabricated through a similar electrodeposition technique, apart from different lower depositing potentials, on a conductive ITO substrate. The resulting NiO materials were characterised by XPS, SEM-EDX and Raman. The characterisation techniques revealed that the NiO film produced at the shorter potential window was shown to display a more disordered material than the NiO made at the larger potential window. Additionally, the latter material showed an increased amount of sulphate, which can be postulated to come from the deposition solution. The electrochromic capabilities of the two NiO materials are encouraging. The coloration efficiency for deposition process 1 and deposition process 2 are 49 and 17 cm² C⁻¹, respectively while the switching time for deposition 1 for coloration and bleaching is 5.7/7.4 seconds. These switching times are faster than previously reported times for other electrodeposited NiO films with similar thicknesses.

ACKNOWLEDGEMENTS

The manuscript was written through contributions of MPB and MEGL. All authors have given approval to the final version of the manuscript. MPB did the spectroelectrochemical analysis and SEM-EDX. MPB and HN did the Raman analysis. MPB and NCB did the XPS. This publication has emanated in part from research conducted with the financial support of Science Foundation Ireland (SFI) under Grant Number SFI/10/IN.1/I2969. We would like to thank the staff in the AML, CRANN for help with the SEM analysis.

References

1. D.S. Dalavi, R.S. Devan, R.S. Patil, Y.-R. Ma, P.S. Patil, *Mater. Lett.*, 90 (2013) 60.
2. X.H. Xia, J.P. Tu, J. Zhang, X.L. Wang, W.K. Zhang, H. Huang, *Sol. Energy Mater. Sol. Cells*, 92 (2008) 628.
3. M. Gómez, A. Medina, W. Estrada, *Sol. Energy Mater. Sol. Cells*, 64 (2000) 297.
4. M.Z. Sialvi, R.J. Mortimer, G.D. Wilcox, A.M. Teridi, T.S. Varley, K.G.U. Wijayantha, C.A. Kirk, *ACS Applied Materials & Interfaces*, 5 (2013) 5675.
5. B. Vidhyadharan, N.K.M. Zain, I.I. Misnon, R.A. Aziz, J. Ismail, M.M. Yusoff, R. Jose, *J. Alloys Compd.*, 610 (2014) 143.

6. J. Xu, L. Gao, J. Cao, W. Wang, Z. Chen, *Electrochim. Acta*, 56 (2010) 732.
7. X.-C. Dong, H. Xu, X.-W. Wang, Y.-X. Huang, M.B. Chan-Park, H. Zhang, L.-H. Wang, W. Huang, P. Chen, *ACS Nano*, 6 (2012) 3206.
8. M.P. Browne, H. Nolan, G.S. Duesberg, P.E. Colavita, M.E.G. Lyons, *ACS Catalysis*, 6 (2016) 2408.
9. M. Browne, R.J. Cullen, R.L. Doyle, P.E. Colavita, M.E.G. Lyons, *ECS Transactions*, 53 (2013) 59.
10. M.E.G. Lyons, R.L. Doyle, D. Fernandez, I.J. Godwin, M.P. Browne, A. Rovetta, *Electrochem. Commun.*, 45 (2014) 56.
11. S. Tao, J.T.S. Irvine, *Nat Mater*, 2 (2003) 320-323.
12. R.J. Gorte, S. Park, J.M. Vohs, C. Wang, 12 (2000) 1465.
13. S.H. Baeck, K.S. Choi, T.F. Jaramillo, G.D. Stucky, E.W. McFarland, *Adv. Mater.*, 15 (2003) 1269.
14. D.T. Gillaspie, R.C. Tenent, A.C. Dillon, *J. Mater. Chem.*, 20 (2010) 9585.
15. M.K. Carpenter, R.S. Conell, D.A. Corrigan, *Solar Energy Mater.*, 16 (1987) 333.
16. J.L. Garcia-Miquel, Q. Zhang, S.J. Allen, A. Rougier, A. Blyr, H.O. Davies, A.C. Jones, T.J. Leedham, P.A. Williams, S.A. Impey, *Thin Solid Films*, 424 (2003) 165.
17. Y. Kazuki, M. Takeshi, T. Sakae, *Japanese Journal of Applied Physics*, 34 (1995) 2440.
18. M.W. Louie, A.T. Bell, *J. Am. Chem. Soc.*, 135 (2013) 12329.
19. D.S. Hall, D.J. Lockwood, S. Poirier, C. Bock, B.R. MacDougall, *The Journal of Physical Chemistry A*, 116 (2012) 6771.
20. A.P. Grosvenor, M.C. Biesinger, R.S.C. Smart, N.S. McIntyre, *Surf. Sci.*, 600 (2006) 1771.
21. S.-H. Lin, F.-R. Chen, J.-J. Kai, *Appl. Surf. Sci.*, 254 (2008) 3357.
22. M.M. Uplane, S.H. Mujawar, A.I. Inamdar, P.S. Shinde, A.C. Sonavane, P.S. Patil, *Appl. Surf. Sci.*, 253 (2007) 9365.
23. S.A. Mahmoud, S.A. Aly, M. Abdel-Rahman, K. Abdel-Hady, *Physica B: Condensed Matter*, 293 (2000) 125.